Spectrochimica Acta Part A: Molecular and Biomolecular Spectroscopy 137 (2015) 581–588

Contents lists available at ScienceDirect

Spectrochimica Acta Part A: Molecular and Biomolecular Spectroscopy

journal homepage: www.elsevier.com/locate/saa

Hg(II)-activated emission “turn-on” chemosensors excited by up-conversion nanocrystals: Synthesis, characterization and sensing performance

Shigang Li [a,*], Xiaoyun Zhao [a], Dongliang Tao [b,*], Wenbao Zhang [b], Kaiyin Zhang [b]

[a] School of Physics and Electronic Science, Fuyang Teachers College, Fuyang, Anhui 236037, China
[b] School of Chemical and Chemical Engineering, Fuyang Teachers College, Fuyang, Anhui 236037, China

HIGHLIGHTS

- Two rhodamine-derived sensing probes for Hg(II) ions were reported.
- An up-conversion host $NaYF_4$ lattice was chosen as the excitation host.
- Energy transfer between the host and the probe were confirmed.
- Emission “turn-on” effect, good selectivity and linear response were observed.

GRAPHICAL ABSTRACT

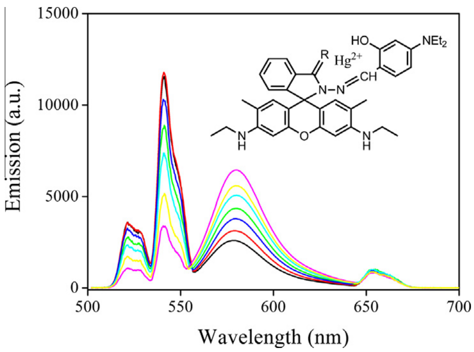

ARTICLE INFO

Article history:
Received 7 July 2014
Received in revised form 7 August 2014
Accepted 24 August 2014
Available online 6 September 2014

Keywords:
Hg(II)
Up-conversion nanocrystals
Sensor
Rhodamine derivative

ABSTRACT

In this paper, two emission “turn-on” chemosensors for Hg(II) sensing were designed and synthesized. Up-conversion $NaYF_4$ nanocrystals were prepared and used as the excitation host for both chemosensors. Spectral analysis suggested that there should be an efficient energy transfer between the host and the chemosensors, which was then confirmed by excited state lifetime analysis. Then two sensing systems using this up-conversion host and the two chemosensors were constructed, their sensing performance for Hg(II) ions was then studied. It was found that the probe emission intensity increased with increasing Hg(II) concentrations, showing an emission “turn-on” effect. Good selectivity and linear response were observed from both sensing systems.

Introduction

Mercury and its compounds are a well-known health hazard for most animal species including human beings [1]. A series of natural and anthropogenic activities can raise Hg contaminations. Those inorganic ones can be accumulated and converted into organic ones by microbes and their food chains, taking more harm to living lives [2]. The desire for reliable indicating and sensing methods has pushed a progress of analytical techniques such as atomic absorption spectroscopy, chemiluminescence and voltammetry [3–5]. Despite of their precise and reliable readings, those techniques are limited for on-line and in-field monitoring since sophisticated apparatus and equipments are needed for those operations [3–5].

Recently, optical sensors have drawn much attention owing to the virtues of quick response and low need for instrumentation [3,4]. In addition, optical sensing signals can be transmitted over a

---

* Corresponding authors.
E-mail addresses: shigangli01@163.com (S. Li), tdlpku@163.com (D. Tao).

http://dx.doi.org/10.1016/j.saa.2014.08.109
1386-1425/

long distance with no electromagnetic interference, making them a promising proposal for on-line and in-field monitoring [5,6]. Some optical sensing systems for Hg(II) detection have been reported [6–8]. Regardless of above mentioned virtues, those systems are generally based on emission "turn-off" probes excited by high energy light, which causes the following two defects. First, limited accuracy and selectivity. The sensing operation of an emission "turn-off" probe is based on probe emission quenching. Since both analyte and other competing species can quench probe emission, a detection error can be encountered upon a complicated environment full of competing species and emission killers. Second, strong background light interference and poor photostability. Under high energy radiation, some coexisting chromophores and fluorophores may be excited simultaneously, leading to background light emission. On the other hand, probes may be photooxidized and decomposed by high energy radiation, namely the poor photostability. Thus, those optical sensing systems should be optimized and adjusted aiming at better analyte recognition and photostability.

It seems that the combination of an emission "turn-on" probe and an up-conversion host can well solve above problems. In this case, an emission "turn-on" probe means that its emission is sensitive to specific analyte but immune to the others, providing high selectivity [8–10]. An up-conversion host can harvest near-IR radiation and emit suitable light for probe excitation, avoiding a direct high energy excitation and thus the background light interference from co-existing chromophores [11,12].

Given above considerations, in this work, two rhodamine derivatives are designed as potential Hg(II) sensing probes owing to their emission "turn-on" character activated by Hg(II) ions [13–16]. An up-conversion $NaYF_4$ lattice is constructed as the excitation host. Their synthetic and construction strategy is shown as Scheme 1. The photophysical characters of the two probes and the excitation host are studied. The Hg(II) sensing performance of their resulting composite system is also investigated.

Experimental details

Reagents and synthesis

The staring reagents used in this work, including rhodamine 6G, hydrazine (95 wt%), Lawesson's reagent, 4-(diethylamino)-2-hydroxybenzaldehyde, Triton X-100, NaOH, HCl, mercury nitrate, rear earth ions and other inorganic metal salts, were purchased from Tianjin Chemical Company (Tianjin, China). The organic solvents, including anhydrous ethanol, acetonitrile and toluene, were purified with standard operations. The solvent water was deionized.

2-amino-3′,6′-bis(ethylamino)-2′,7′-dimethylspiro[isoindoline-1,9′-xanthen]-3-one (denoted as 2). 2 was synthesized by the following procedure [17]. Rhodamine 6G (2 g) and anhydrous hadrazine (10 mL) were dissolved in ethanol (30 mL) and heated to reflux under N_2 atmosphere for 12 h. Then the solution was cooled and poured into plenty of cold water. The resulting solid sample was collected and recrystallized in a mixed solvent of ethanol/water (V/V = 4:6) to give 2 as yellow solid. ^1H NMR ($CDCl_3$), δ (ppm): 1.27–1.33 (t, 6H, $NCH_2\mathit{CH_3}$), 1.95 (s, 6H, xanthene-$\mathit{CH_3}$), 3.22–3.27 (q, 4H, $N\mathit{CH_2}CH_3$), 4.81 (s, N—$\mathit{NH_2}$), 5.36 (s, $\mathit{NH}CH_2CH_3$), 6.18 (s, 2H, xanthene-H), 6.45 (s, 2H, xanthene-H), 7.16 (dd, 1H, Ar—H), 7.55 (dd, 2H, Ar—H), 8.24 (dd, 1H, Ar—H). MS m/z: $[m + 1]^+$ calc. for $C_{26}H_{28}N_4O_2$, 428.2; found, 429.2.

2-amino-3′,6′-bis(ethylamino)-2′,7′-dimethylspiro [isoindoline-1,9′-xanthene]-3-thione (denoted as 3). 3 was synthesized by the following procedure [18]. 2 (5 mmol) and Lawesson's reagent (7 mmol) were dissolved in anhydrous toluene (40 mL) and heated to reflux under N_2 atmosphere for 6 h. The solvent was then removed by rotary evaporation. The crude product was purified on a silica column with CH_2Cl_2 as eluent to give 3 as light red solid. ^1H NMR ($CDCl_3$), δ (ppm): 1.28–1.35 (t, 6H, $NCH_2\mathit{CH_3}$), 1.96 (s, 6H, xanthene-$\mathit{CH_3}$), 3.24–3.28 (q, 4H, $N\mathit{CH_2}CH_3$), 4.76 (s, N—$\mathit{NH_2}$), 5.35 (s, $\mathit{NH}CH_2CH_3$), 6.17 (s, 2H, xanthene-H), 6.46 (s, 2H, xanthene-H), 7.17 (dd, 1H, Ar—H), 7.55 (dd, 2H, Ar—H), 8.24 (dd, 1H, Ar—H). MS m/z: $[m + 1]^+$ calc. for $C_{26}H_{28}N_4OS$, 444.2; found, 445.2.

2-((4-(diethylamino)-2-hydroxybenzylidene) amino)-3′,6′-bis (ethylamino)-2′,7′- dimethylspiro [isoindoline-1,9′-xanthen]-3-one (denoted as 4). 4 was synthesized by the following procedure [18]. 2 (1 mmol) and 4-(diethylamino)-2-hydroxybenzaldehyde (1 mmol) were dissolved in ethanol (30 mL) and heated to reflux for 12 h under N_2 atmosphere. The solvent was then removed by rotary evaporation. The crude product was purified on a silica column with CH_2Cl_2 as eluent to give 4 as yellow solid. ^1H NMR ($CDCl_3$), δ (ppm): 1.13–1.18 (t, 6H, $NCH_2\mathit{CH_3}$), 1.26–1.32 (t, 6H, $NCH_2\mathit{CH_3}$), 1.95 (s, 6H, xanthene-$\mathit{CH_3}$), 3.12–3.17 (q, 4H, $N\mathit{CH_2}CH_3$),

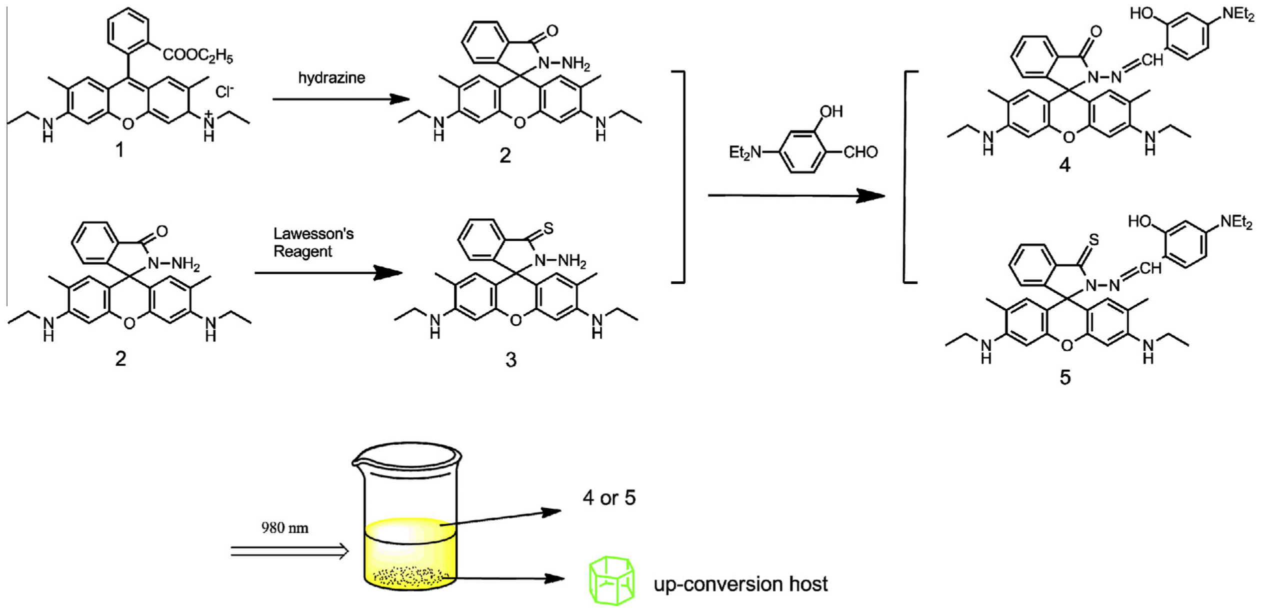

Scheme 1. The synthetic route for the two chemosensors, along with the depiction for the Hg(II) sensing systems.

3.22–3.26 (q, 4H, $\mathrm{N}CH_2\mathrm{CH}_3$), 5.32 (s, $NH\mathrm{CH}_2\mathrm{CH}_3$), 6.03 (s, 1H, Ar—H), 6.11 (d, 1H, Ar—H), 6.17 (s, 2H, xanthene-H), 6.44 (s, 2H, xanthene-H), 7.17 (dd, 1H, Ar—H), 7.32 (d, 1H, Ar—H), 7.58 (dd, 2H, Ar—H), 8.26 (dd, 1H, Ar—H), 8.41 (s, 1H, CH═N), 9.12 (s, Ar—OH). ^{13}C NMR ($CDCl_3$), δ (ppm): 13.33, 14.49, 16.86, 35.24, 46.37, 75.87, 98.32, 99.94, 103.37, 106.39, 113.45, 118.35, 127.39, 127.78, 129.01, 129.64, 131.54, 132.74, 132.80, 138.87, 143.26, 143.35, 148.69, 153.34, 164.32, 171.12. MS *m*/*z*: $[\mathrm{m}+1]^+$ calc. for $C_{37}H_{41}N_5O_3$, 603.8; found, 604.8. Melting point: 212–215 °C.

2-((4-(diethylamino)-2-hydroxybenzylidene) amino)-3′,6′-bis(ethylamino)-2′,7′-dimethylspiro[isoindoline-1,9′-xanthene]-3-thione (denoted as 5). 5 was synthesized following a similar procedure for 4, except that 2 was replaced by 3. ^{1}H NMR ($CDCl_3$), δ (ppm): 1.15–1.19 (t, 6H, NCH_2CH_3), 1.28–1.33 (t, 6H, NCH_2CH_3), 1.93 (s, 6H, xanthene-CH_3), 3.11–3.16 (q, 4H, $\mathrm{N}CH_2\mathrm{CH}_3$), 3.20–3.25 (q, 4H, $\mathrm{N}CH_2\mathrm{CH}_3$), 5.32 (s, $NH\mathrm{CH}_2\mathrm{CH}_3$), 6.05 (s, 1H, Ar—H), 6.13 (d, 1H, Ar—H), 6.19 (s, 2H, xanthene-H), 6.45 (s, 2H, xanthene-H), 7.18 (dd, 1H, Ar—H), 7.31 (d, 1H, Ar—H), 7.59 (dd, 2H, Ar—H), 8.27 (dd, 1H, Ar—H), 8.44 (s, 1H, CH═N), 9.14 (s, Ar—OH). ^{13}C NMR ($CDCl_3$), δ (ppm): 13.78, 14.61, 16.93, 36.12, 46.52, 79.95, 98.14, 99.18, 104.65, 106.62, 113.27, 118.47, 124.67, 126.32, 129.78, 130.25, 131.17, 132.84, 141.56, 141.69, 143.12, 143.31, 148.79, 153.41, 161.92, 169.31. MS *m*/*z*: $[\mathrm{m}+1]^+$ calc. for $C_{37}H_{41}N_5O_2S$, 619.8; found, 620.8. Melting point: 216–219 °C.

Up-conversion host

The up-conversion host β-$NaYF_4$:Yb^{3+}/Er^{3+} was synthesized by the following procedure [8]. The solution of NaOH (17 mmol), NaF solution (0.8 M, 10 mL), oleic acid (7 g) and ethanol (12 mL) was stirred and aged at room temperature for 30 min. After the addition of $Yb(NO_3)_3$ solution (0.2 M, 1 mL), $Y(NO_3)_3$ solution (0.4 M, 2 mL) and $Er(NO_3)_3$ solution (0.01 M, 2 mL), the mixture was held still for 30 min and then sealed into a Teflon bottle. The mixture was heated to 200 °C and kept for 10 h (heating rate = 10 °C/min). After being cooled naturally, the solid product was collected and dispersed in Triton X-100 (30 mL). The mixture was processed with ultrasonic bath for 20 min. The solid product was collected by centrifugation, washed and dried to give the up-conversion host β-$NaYF_4$:Yb^{3+}/Er^{3+}.

Sensing system

A typical sensing system was constructed as follows. A controlled amount of β-$NaYF_4$:Yb^{3+}/Er^{3+} was added into 1 L of NaAc–HAc buffer solution (pH = 7)/CH_3CN (V:V = 1:1) to form a 5 wt% solution. Then chemosensor (0.01 mmol) was added. The solution was treated with ultrasonic bath for 10 min for further measurements.

Equipments

The equipments and measuring methods used in this work are listed as follows. NMR and mass spectra were taken by a Varian INOVA 300 spectrometer and a Agilent 1100 MS spectrometer (COMPACT), respectively. Melting point measurement as finished on a MPA100 (SRS) melting-pint apparatus. Scanning and transmission electron microscopy (SEM and TEM) images were shot by a Hitachi S-4800 microscope and a JEM-2010 transmission election microscope (Japanese JEOL Company), respectively. Energy-dispersive X-ray (EDX) data were taken simultaneously by the JEM-2010. UV–Vis absorption and fluorescence emission spectra were recorded by a Hitachi UV-3110PC UV–VIS-NIR scanning spectrophotometer and a Hitachi F-4500 fluorescence spectrophotometer, respectively. The excited state lifetimes were recorded by a two-channel TEKTRONIX TDS-3052 oscilloscope. Above photophysical measurements were recorded using sample suspensions in NaAc–HAc buffer (pH = 7)/CH_3CN (V:V = 1:1). A tunable laser was used as the excitation source (Continuum Sunlite OPO) (λ = 980 nm).

Results and discussion

Characterization on up-conversion host

To minimize background light interference and probe photobleaching, an up-conversion host is selected as the excitation source, as above mentioned. $NaYF_4$ lattice has been proved as a promising one owing to its high up-conversion efficiency [11]. During host preparation procedure, to allow a fast growth along [001] crystallographic direction and obtain hexagonal prism-liked crystals, concentrated rare earth and NaF solutions were used to facilitate the dissolution–reconstruction process, where oleic acid served as a stabilizing reagent. Considering that the resulting nanocrystals were covered by hydrophobic oleic acid chains, they were later treated by an amphiphilic surfactant of Triton X-100 so that the crystals became hydrophilic and dispersible in aqueous solutions.

A hexagonal prism-liked morphology with mean diameter of 20 nm can be identified by the SEM and TEM images of the nanocrystals (Triton X-100 processed), as shown in Fig. S1 (see Supporting information). Their composition can be firstly revealed by the EDX data shown in Fig. 1. There are C, F, Na, Er, Yb and Y elements in the nanocrystals, which is consistent with our proposed composition. The existence of C element suggests that there may be some remaining X-100 or oleic acid attached to the nanocrystals. As shown in Fig. 2, the powder XRD pattern of the nanocrystals (Triton X-100 processed) is nearly identical to that of pure hexagonal $NaYF_4$ nanocrystals (JCPDS card No. 28-1192). There can be found no other diffraction peaks, suggesting that the $NaYF_4$ lattice has been preserved well after the incorporation of Yb(III) and Er(III) ions. Considering above results, it can be concluded that the up-conversion host β-$NaYF_4$:Yb^{3+}/Er^{3+} has been successfully constructed.

Photophysical measurement on the host and the two chemosensors

Emission and absorption spectra

Since β-$NaYF_4$:Yb^{3+}/Er^{3+} nanocrystals are designed as the excitation host, the possibility of energy transfer between β-$NaYF_4$:Yb^{3+}/Er^{3+} and the two chemosensors should be considered. First, their absorption and emission spectra are shown in Fig. 3 for comparison. The up-conversion host owns three major bands peaking at 522 nm, 541 nm and 653 nm, respectively. Those bands can be assigned to

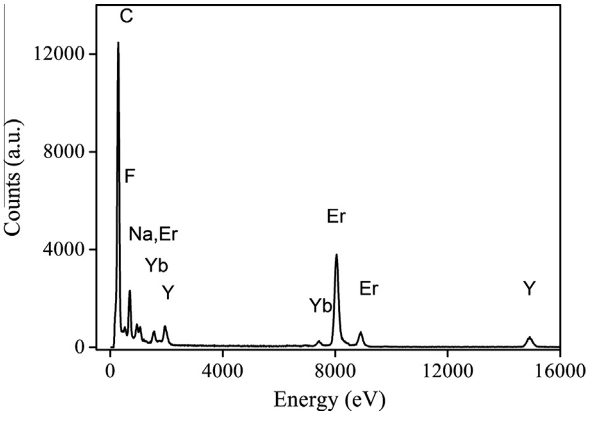

Fig. 1. The EDX data of the host nanocrystals (Triton X-100 processed).

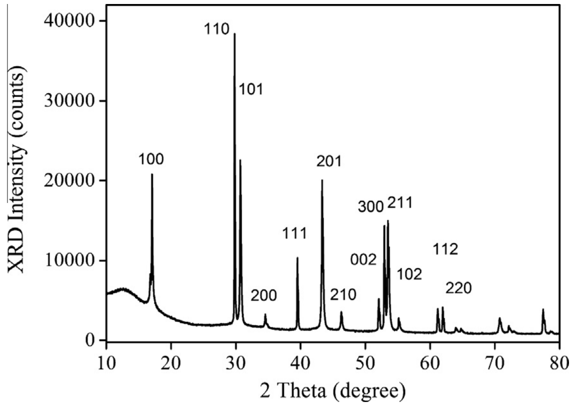

Fig. 2. The powder XRD pattern of the host nanocrystals (Triton X-100 processed).

Er(III) electronic transitions of $^2H_{11/2} \rightarrow {}^4I_{15/2}$, $^4S_{3/2} \rightarrow {}^4I_{15/2}$ and $^4F_{9/2} \rightarrow {}^4I_{15/2}$, suggesting that the up-conversion host has been prepared successfully. The absorption and emission spectra of 4 are quite similar to those of 5, clearly owing to their similar molecular structures. It is observed that the absorption spectra of 4 and 5 overlap well with the up-conversion emission bands, suggesting a possible energy transfer between the up-conversion host and the two chemosensors. In the presence of Hg(II) ions, the two chemosensors exhibit bright emissions peaking at 574 nm for 4 and 580 nm for 5, respectively. Here, Hg(II) ions are introduced to make the two chemosensors take the emissive xanthene structure instead of the non-emissive spirolactam one [13–16].

Sensing mechanism and association constants

Although above emission spectra has convinced that Hg(II) ions can activate the xanthene structure, a detailed analysis on the binding stoichiometry between Hg(II) and chemosensors should be done. Fig. 4 shows the Job's plots of 4:Hg(II) and 5:Hg(II) systems, where the total [Hg(II) + 4/5] amount is maintained as 10 μM and Hg(II) molar fraction increases from 10% to 90%. The emission intensity firstly increases with the increasing Hg(II) concentration, showing the highest emission intensity at Hg(II) molar fraction of 50%. Then the emission intensity decreases with the increasing Hg(II) concentration. This finding suggests a simple complexation ratio of 1:1, as exhibited by Formula (1), where K_s means association constant. Here, K_s can be calculated by Formula (2) and Formula (3), where A_T and A_0 means the critical absorbance values when $\alpha = 1$ (fully coordinated with Hg(II)) and $\alpha = 0$ (no Hg(II))

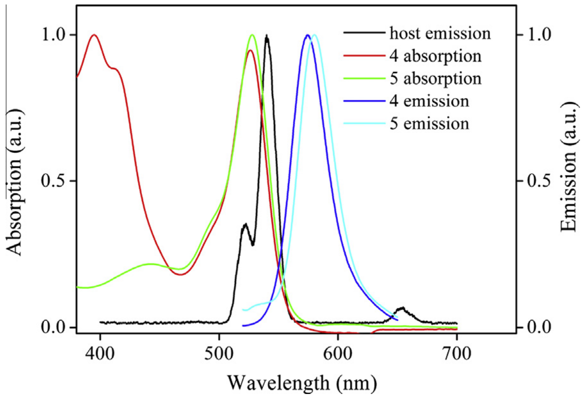

Fig. 3. The absorption and emission (λ_{ex} = 525 nm) spectra of 4 and 5 (10 μM) admixed with 1 eq. Hg(II) and the up-conversion emission of host nanocrystals in NaAc–HAc buffer (pH = 7)/CH$_3$CN (V:V = 1:1) (5 wt%, λ_{ex} = 980 nm).

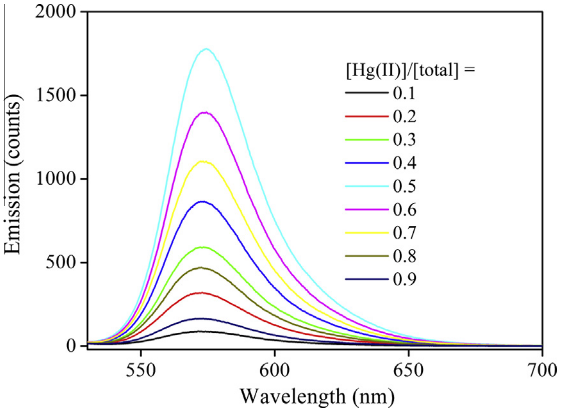

Fig. 4A. The emission spectra of 4:Hg(II) in NaAc–HAc buffer solution (pH = 7)/CH$_3$CN (V:V = 1:1, λ_{ex} = 525 nm), where the total [Hg(II) + 4] amount is adjusted as 10 μM and the Hg(II) molar fraction increases from 10% to 90%.

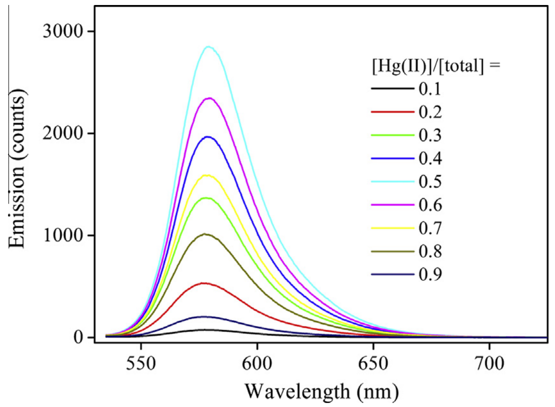

Fig. 4B. The emission spectra of 5:Hg(II) in NaAc–HAc buffer solution (pH = 7)/CH$_3$CN (V:V = 1:1, λ_{ex} = 525 nm), where the total [Hg(II) + 5] amount is adjusted as 10 μM and the Hg(II) molar fraction increases from 10% to 90%.

$$\text{Chemosensor} + \text{Hg(II)} \overset{K_s}{\leftrightarrow} \text{chemosensor} : \text{Hg(II)} \tag{1}$$

$$\frac{\alpha}{1-\alpha} = \frac{1}{K_s[\text{Hg(II)}]} \tag{2}$$

$$\alpha = \frac{A_T - A}{A_T - A_0} \tag{3}$$

The association constants are determined as $2.46 \times 10^3\ M^{-1}$ for 4:Hg(II) and $4.12 \times 10^3\ M^{-1}$ for 5:Hg(II), respectively, as shown by Fig. 5. It is observed that 5 owns a higher affinity to Hg(II) ions than 4 does, owing to the strong interaction between S atom in 5 and Hg(II) ions. These values, however, are obviously lower with literature values, which may be explained by the steric hindrance in 4 and 5 [18].

Energy transfer radius and efficiency

Regardless of the spectral overlap between β-NaYF$_4$:Yb^{3+}/Er^{3+} emission and 4/5 absorption, the Forster radius between them should be considered. Forster radius is defined as the effective distance between a donor–acceptor pair, as depicted by Formula (4) [19]. Here Q_0 means the intrinsic donor emission yield of β-NaYF$_4$:Yb^{3+}/Er^{3+} which has been reported as 3% [20]. J is the overlap integral between donor emission and acceptor absorption, κ^2 is mutual molecular orientation factor, N_A is Avogadro number and n_d is solvent refraction index, respectively.

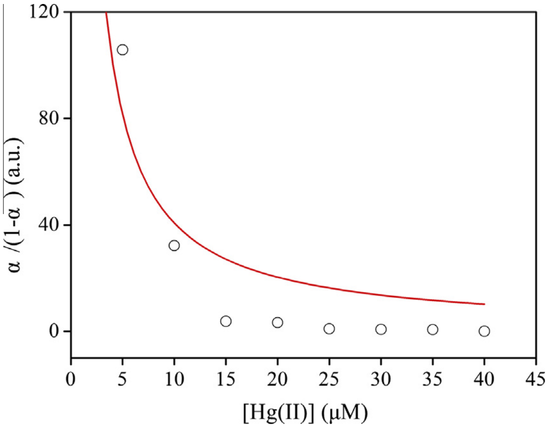

Fig. 5A. The fitting plots for Formula (2) of 4 in NaAc–HAc buffer solution (pH = 7)/CH_3CN (V:V = 1:1) (40 μM) when Hg(II) concentration increases from 5 μM to 40 μM.

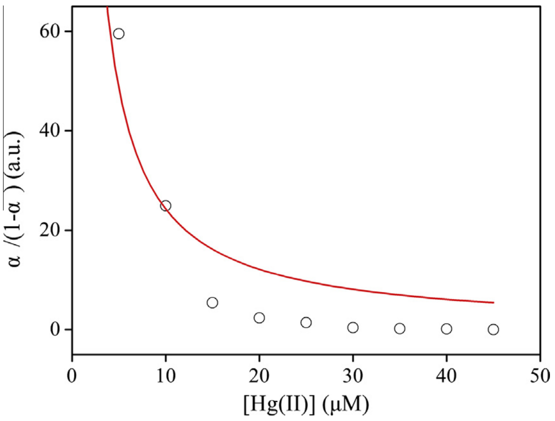

Fig. 5B. The fitting plots for Formula (2) of 5 in NaAc–HAc buffer solution (pH = 7)/CH_3CN (V:V = 1:1) (40 μM) when Hg(II) concentration increases from 5 μM to 45 μM.

$$R_0^6 = \frac{9Q_0k^2J(\ln 10)}{128\pi^5 n_d^4 N_A} \tag{4}$$

$$J = \int f_D(\lambda)\varepsilon_A(\lambda)\lambda^4\,d\lambda \tag{5}$$

Based on the spectra in Fig. 3, the R_0 values are calculated as 19 Å for host:4 and 22 Å for host:5, respectively. Both Forester radii are slightly shorter than literature values, suggesting that a high concentration of host:chemosensor mixture is needed to guarantee an efficient energy transfer between them [21–24].

In order to finally confirm the energy transfer between the host and the chemosensors, the emission decay lifetime variation of β-$NaYF_4$:Yb^{3+}/Er^{3+} (Er^{3+}, $^4S_{3/2}$) is investigated upon the presence or absence of the chemosensors. Similarly, Hg(II) ions are added to maintain the xanthene structure. As shown in Fig. 6, the intrinsic host owns a long emission decay lifetime of 204 μs. Upon the addition of the two chemosensors, the lifetimes slightly decrease to 184 μs for host:4 system and 187 μs for host:5 system, respectively. Here, the energy transfer between the host and the chemosensor is weak, which means that the non-emissive spirolactam structure is ineffective on adsorbing host energy [13,15,16]. In the presence of Hg(II) ions, a xanthene structure is triggered. Correspondingly, the lifetimes decreases obviously to 75 μs for host:4 system and 128 μs for host:5 system, respectively. Thus, efficient energy transfer between the host and the chemosensors can be established. Energy transfer efficiency (η) values in both systems can be calculated as 59.2% and 31.6% according to Formula (6), where τ is $^4S_{3/2}$ excited state lifetime of host:chemosensor system, τ' is that of host:chemosensor:Hg(II) system [7,8]. It seems that the energy transfer in host:4 system is more efficient than that in host:5 system, owing to their matched emission and absorption spectra.

$$\eta = 1 - \tau'/\tau \tag{6}$$

Sensing performance of host:chemosensor systems

Spectral response

The sensing performance of host:chemosensor systems is firstly analyzed by their emission spectra upon increasing Hg(II) concentrations, as shown in Fig. 7. In the absence of Hg(II) ions, three up-conversion emissions peaking at 522 nm, 541 nm and 653 nm are observed. In addition, there are weak emissions from the chemosensors peaking at 575 nm in host:4 system and 580 nm in host:5 system. Upon increasing Hg(II) concentrations, the former two up-conversion emissions gradually decrease their intensity. Meanwhile, the emissions from both chemosensors are greatly enhanced, showing an emission “turn-on” effect triggered by Hg(II) ions. On the other hand, the third up-conversion emission peaking at 653 nm remains constant under various Hg(II) concentrations. This phenomenon can be well explained by the fact that there is no effective overlap between this up-conversion emission and chemosensors absorption. In this case, the third up-conversion emission intensity can be applied as an internal reference to understand the energy transfer between host and chemosensors. In other words, the first two up-conversion emissions transfer their energy to the chemosensors, while, the third one could not finish this procedure due to the poor spectral overlap. Since the third up-conversion emission intensity remains constant, the decreased emission intensity of the former two up-conversion emissions can be attributed to the energy transfer to the chemosensors. It is thus confirmed that the exists an efficient energy transfer between the host and both chemosensors. Up-conversion hosts usually suffer from limited efficiency, including ours. Later efforts should be devoted to efficiency improvement. On the other hand, our up-conversion emission and probe emission were all strong enough to be recorded by a fluorescence spectrophotometer. Thus, regardless of their limited efficiency, valid signals can be harvested, with low background light interference.

The emission “turn-on” behavior can be expressed by Stern–Volmer plots and Formula (7) shown by the insets of Fig. 7, where I is probe emission intensity, [Hg(II)] suggests Hg(II) concentration, K_{sv} is Stern–Volmer constant, 0 means the value when [Hg(II)] = 0.

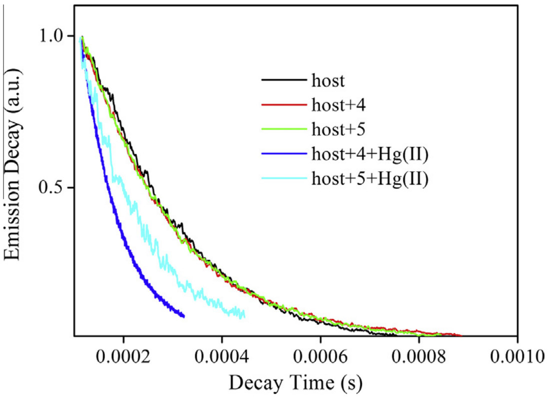

Fig. 6. Excited state decay dynamics of host nanocrystals (Er^{3+}, $^4S_{3/2}$, λ_{ex} = 980 nm) in NaAc–HAc buffer solution (pH = 7)/CH_3CN (V:V = 1:1, 5 wt%) upon the presence or absence of 4/5 (10 μM) and Hg(II) ions (10 μM).

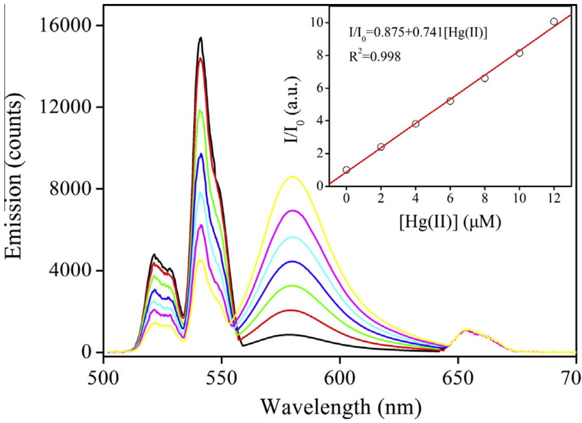

Fig. 7A. The emission spectra of host (5 wt%):4 (10 μM) in NaAc–HAc buffer solution (pH = 7)/CH$_3$CN (V:V = 1:1) upon increasing Hg(II) concentrations (λ_{ex} = 980 nm). Inset: the corresponding Stern–Volmer plots of these spectra.

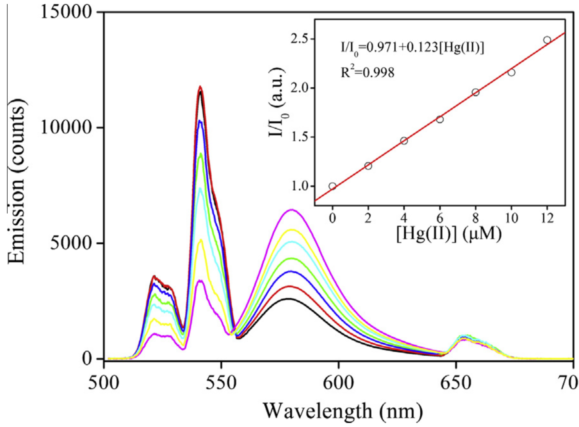

Fig. 7B. The emission spectra of host (5 wt%):5 (10 μM) in NaAc–HAc buffer solution (pH = 7)/CH$_3$CN (V:V = 1:1) upon increasing Hg(II) concentrations (λ_{ex} = 980 nm). Inset: the corresponding Stern–Volmer plots of these spectra.

$$I/I_0 = 1 + K_{sv}[\mathrm{Hg(II)}] \qquad (7)$$

Both systems possess linear response towards increasing Hg(II) concentrations, so that the quantification with these working plots can be easily performed. Molecular structures of 4 and 5 are similar to each other. It seems that replacing O atom in 4 by Lawesson's reagent has no obvious effect on Stern–Volmer linearity. Linear Stern–Volmer curves have also been obtained in homogeneous medium for similar systems [8,16,18]. On the other hand, covalent grafting between probe and supporting matrix/host usually gives non-linear Stern–Volmer curves [12,13,22,24]. We thus come to a conclusion that Stern–Volmer linearity depends mainly on the microenvironment around probe molecules: a homogeneous one gives linear Stern–Volmer response, while an inhomogeneous one causes poor linearity. Here, limit of detection (LOD) is defined as the Hg(II) concentration when I/I_0 value is equal to 1.1. With above linear Stern–Volmer curves, LOD values are obtained as 0.3 μM for host:4 system and 1.0 μM for host:5 system, respectively. Given the same Hg(II) concentration (>0), host:4 system owns a higher I/I_0 value than host:5 system does. This can be explained by the high I_0 value in host:5 system. To improve its sensitivity, the intrinsic emission intensity in host:5 should be decreased to minimal level.

Emission signal stability and selectivity

Since above sensing and quantification procedure is based on emission intensity measurement, the emission stability under continuous radiation should be considered [11,12,25]. Fig. 8A shows the emission intensity variations of host:4 and host:5 systems under continuous radiation. It is observed that the probe emission intensity of both systems obviously decreases with increasing radiation time. On the other hand, the up-conversion emission peaking at 653 nm is greatly maintained. As shown by the inset of Fig. 8A, the emission intensities of 4:Hg(II) and 5:Hg(II) systems can be well maintained within 10 h, suggesting that the probes and their adducts with Hg(II) ions are stable. Thus, the decreased probe emission is mainly caused by the photobleaching of probes themselves (or their adducts with Hg(II) ions). In other words, the inorganic NaYF$_4$ based host is stable under 980 nm radiation with constant up-conversion output, while, 4, 5 and their Hg(II)-adducts may not be stable enough under continuous up-conversion excitation.

Generally, rhodamine based emission is usually sensitive towards pH variation. Thus, pH response of host:chemosensors:Hg(II) sensing systems is recorded and shown in Fig. 8B. It is observed that the sensing emission increases with decreasing pH values, which may be explained as follows. In acid medium, excess protons can partially trigger the emission "turn-on" process, showing increased emission [8,12]. In alkaline medium, the emission "turn-on" process is reversed by decreasing protons. In addition, free Hg(II) tends to precipitate as HgO, which also reverses the emission "turn-on" process, showing decreased emission. Aiming at reliable and accurate data, sensing operations should be performed in buffer solutions to minimize pH interference.

Selectivity has been defined as the recognizing ability of a probe for specific analyte in a complicated environment full of competing species [11,12,25]. Good selectivity is usually desired from most sensing systems. The spectral response of both systems towards some common metal ions is thus determined and shown as Fig. 9. No surprise, the presence of Hg(II) ions can activate the emission "turn-on" effect. Due to its similar ionic radius and charge to those of Hg(II), Cu(II) ions can partially activate the emission "turn-on" effect, which means that Cu(II) ions can coordinate with the chemosensors and make them take the delocalized xanthene structure. However, the partially-filled d orbitals of Cu(II) ions quench the probe emission. Thus, its emission "turn-on" effect is not as obvious as Hg(II)'s. It seems that 5 is more sensitive towards Cu(II) ions than 4 does, which may be attributed to the strong S—Cu interaction between 5 and Cu(II) ions.

As for the other studied metal ions, including Na(I), Mg(II), Al(III), K(I), Ca(II), Co(II), Zn(II), Cd(II) and Ag(I) ions, they are nearly

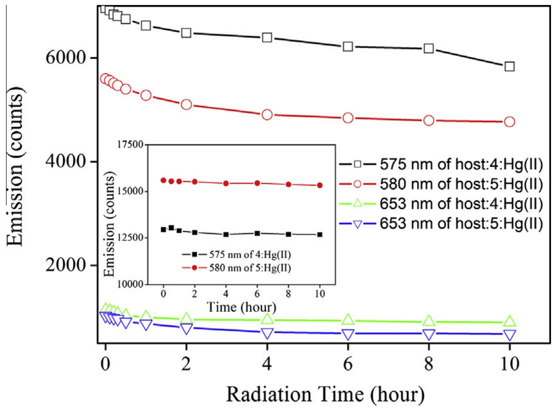

Fig. 8A. The emission intensity variation of host (5 wt%):chemosensors (10 μM):Hg(II) (10 μM) sensing systems in NaAc–HAc buffer solution (pH = 7)/CH$_3$CN (V:V = 1:1) upon continuous radiation (λ_{ex} = 980 nm). Inset: the emission intensity variation of chemosensors (10 μM):Hg(II) (10 μM) in NaAc–HAc buffer solution (pH = 7)/CH$_3$CN (V:V = 1:1) upon interval radiation (λ_{ex} = 525 nm).

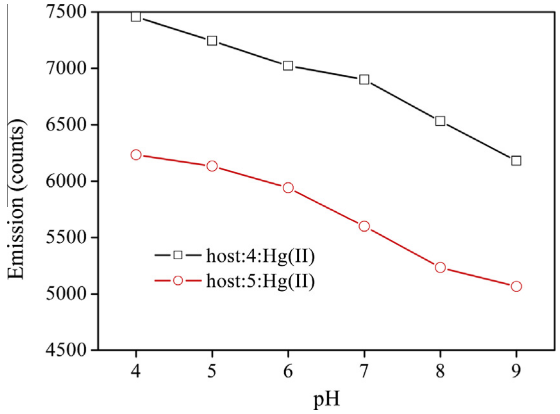

Fig. 8B. PH response of host (5 wt%):chemosensors (10 μM):Hg(II) (10 μM) sensing systems (λ_{ex} = 980 nm).

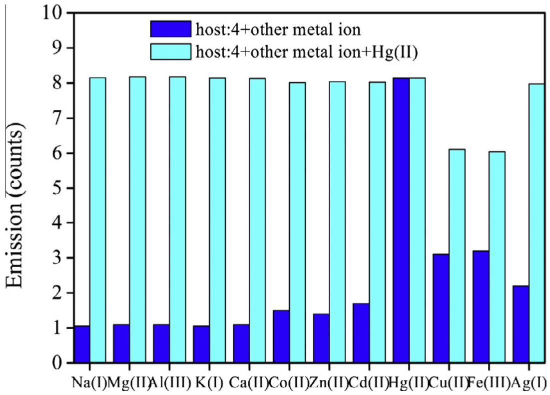

Fig. 9A. The emission intensities of host (5 wt%):4 (10 μM) sensing systems in NaAc–HAc buffer solution (pH = 7)/CH_3CN (V:V = 1:1, λ_{ex} = 980 nm) upon various metal ions (10 μM).

irrelevant to the probe emission “turn-on” effect. We are giving a tentative explanation as follows. As mentioned above, free rhodamine derivatives usually take the spirolactam structure (non-emissive). Given proper coordination center, the probe molecules take the xanthene structure which is highly emissive, showing the emission “turn-on” effect [13]. Owing to the high thermodynamic affinity for N,O-chelate ligands and fast metal-to-ligand binding kinetics, Hg(II) ions are highly effective on activating the emission “turn-on” effect of 4 and 5 [26]. Cu(II) ions own similar ionic radius and charge to those of Hg(II) and thus can also trigger the structural transformation from spirolactam one to xanthene one. However, the emission “turn-on” effect is compromised by the partially-filled d orbitals. As for the other metal ions, they may fail to match the coordination caves in 4 and 5. With the structural transformation missing, it is reasonable to see probes' immunity to them. Thus, it can be concluded that both sensing systems own good selectivity towards common metal ions. This finding shows a good example for sensing systems with high selectivity [11,12,25].

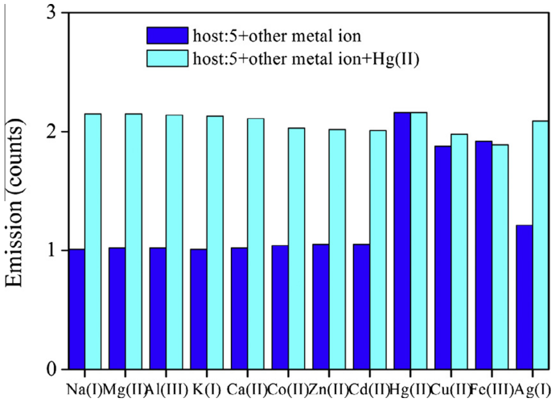

Fig. 9B. The emission intensities of host (5 wt%):5 (10 μM) sensing systems in NaAc–HAc buffer solution (pH = 7)/CH_3CN (V:V = 1:1, λ_{ex} = 980 nm) upon various metal ions (10 μM).

Conclusion

All in all, we proposed two Hg(II) sensing systems using up-conversion β-$NaYF_4$:Yb^{3+}/Er^{3+} nanocrystals as the excitation host and two rhodamine derived molecules as the probes. The excitation host was observed as hexagonal prism-liked crystals and characterized by XRD analysis. Its up-conversion emission spectrum overlapped well with the absorption spectra of the two chemosensors, suggesting a possible energy transfer between the host and the chemosensors. This hypothesis was then confirmed by the excited state lifetime comparison before and after the addition of the two chemosensors. The detailed Hg(II) sensing performance of both sensing systems gave good selectivity and linear working plots, making them promising candidates. For further improvements, the selectivity should be increased. The chemosensors and the excitation host should be embedded into a solid supporting matrix to allow smooth analyte diffusion and to prevent probe leakage.

Acknowledgements

This research was supported by the National Natural Science Foundation of China (Nos. 50973003 and 51271059) and the Natural Science Foundation of Fuyang Normal College (No. 2014FSKJ05ZD).

Appendix A. Supplementary material

Supplementary data associated with this article can be found, in the online version, at http://dx.doi.org/10.1016/j.saa.2014.08.109.

References

[1] M. Nendza, T. Herbst, C. Kussatz, A. Gies, Chemosphere 35 (1997) 1875–1885.
[2] A. Renzoni, F. Zino, E. Franchi, Environ. Res. 77 (1998) 68–72.
[3] Y.A. Vil'pan, I.L. Grinshtein, A.A. Akatove, S. Gucer, J. Anal. Chem. 60 (2005) 38–44.
[4] E. Kopysc, K. Pyrzynska, S. Garbos, E. Bulska, Anal. Sci. 16 (2000) 1309–1312.
[5] L. Yu, X. Yan, Atom. Spectrosc. 25 (2004) 145–153.
[6] L. Zhang, B. Li, Z. Su, S. Yue, Sensor Actuat. B – Chem. 143 (2010) 595–599.
[7] L. Zhang, B. Li, Spectrochim. Acta A 74 (2009) 1060–1063.
[8] J. Zhang, B. Li, L. Zhang, H. Jiang, Chem. Commun. 48 (2012) 4860–4862.
[9] H. Kim, M. Achermann, L.P. Balet, J.A. Hollingsworth, V.I. Klimov, J. Am. Chem. Soc. 127 (2005) 544–546.
[10] Z.Y. Liu, G.S. Yi, H.T. Zhang, J. Ding, Y.M. Zhang, J.M. Xue, Chem. Commun. 6 (2008) 694–696.
[11] Z.Q. Li, Y. Zhang, Angew. Chem. Int. Ed. 45 (2006) 7732–7735.
[12] Y. Yang, B. Li, L. Zhang, P. Li, H. Jiang, Talanta 115 (2013) 938–942.
[13] T. Nguyen, M.B. Francis, Org. Lett. 5 (2003) 3245–3248.
[14] S. Saha, M.U. Chhatbar, P. Mahato, L. Praveen, A.K. Siddhanta, A. Das, Chem. Commun. 48 (2012) 1659–1661.
[15] S. Saha, P. Mahato, G.U. Reddy, E. Suresh, A. Chakrabarty, M. Baidya, S.K. Ghosh, A. Das, Inorg. Chem. 51 (2012) 336–345.
[16] M. Suresh, S. Mishra, S.K. Mishra, E. Suresh, A.K. Mandal, A. Shrivastav, A. Das, Org. Lett. 11 (2009) 2740–2743.
[17] L. He, Z. Li, J. Fu, F. Wang, C. Ma, Y. Deng, Z. Shi, H. Wang, N. He, J. Nanosci. Nanotechnol. 11 (2011) 2256–2262.
[18] Y. Wang, Y. Huang, B. Li, L. Zhang, H. Song, H. Jiang, J. Gao, RSC Adv. 1 (2011) 1294–1300.

[19] A. Kawski, Excitation energy transfer and its manifestation in isotropic media, Photochem. Photobiol. 38 (1983) 487–508.
[20] J.C. Boyer, F. van Veggel, Nanoscale 2 (2010) 1417–1419.
[21] T. Xie, Q. Liu, W.P. Cai, Z. Chen, Y.Q. Li, Chem. Commun. 22 (2009) 3190–3192.
[22] L. Johansson, J. Karolin, J. Chem. Soc., Faraday Trans. 89 (1993) 49–54.
[23] L.S. Sun, H. Peng, M.I.J. Stich, D. Achatz, O.S. Wolfbeis, Chem. Commun. 33 (2009) 5000–5002.
[24] J. Liu, Y. Liu, Q. Liu, C. Li, L. Sun, F. Li, J. Chem. Soc. 133 (2011) 15276–15279.
[25] L. Zhang, S. Yue, B. Li, D. Fan, Inorg. Chim. Acta 384 (2012) 225–232.
[26] R. Krämer, Angew. Chem. Int. Ed. 37 (1998) 772–773.